Pediatric Posterior Fossa Medulloblastoma: The Role of Diffusion Imaging in Identifying Molecular Groups

Nihaal Reddy, David W. Ellison, Bruno P. Soares, Kathryn A. Carson, Thierry A. G. M. Huisman, Zoltan Patay

From the Division of Pediatric Radiology and Pediatric Neuroradiology, Russell H. Morgan Department of Radiology and Radiological Science, Johns Hopkins University School of Medicine, Baltimore, MD (NR, BPS, TAGMH); Department of Pathology, St. Jude Children's Research Hospital, Memphis, TN (DWE); Division of Neuroradiology, Department of Radiology and Imaging Sciences, Emory University School of Medicine, Atlanta, GA (BPS); Department of Epidemiology, Johns Hopkins Bloomberg School of Public Health, Baltimore, MD (KAC) and; and Department of Diagnostic Imaging, St. Jude Children's Research Hospital, Memphis, TN (ZP).

ABSTRACT

BACKGROUND AND PURPOSE: The molecular groups WNT activated (WNT), Sonic hedgehog activated (SHH), group 3, and group 4 are biologically and clinically distinct forms of medulloblastoma. We evaluated apparent diffusion coefficient (ADC) values' utility in differentiating/predicting medulloblastoma groups at the initial diagnostic imaging evaluation and prior to surgery.

METHODS: We retrospectively measured the ADC values of the enhancing, solid portion of the tumor (EST) and of the whole tumor (WT) and performed Kruskal-Wallis testing to compare the absolute tumor ADC values and cerebellar and thalamic ratios of three medulloblastoma groups (WNT, SHH, and group 3/group 4 combined).

RESULTS: Ninety-three children (65 males) were included. Fifty-seven children had group 3/group 4, 27 had SHH, and 9 had WNT medulloblastomas. The median absolute ADC values in the EST and WT were .719 × 10^{-3} and .864 × 10^{-3} mm^2/s for group 3/group 4; .660 × 10^{-3} and .965 × 10^{-3} mm^2/s for SHH; and .594 × 10^{-3} and .728 × 10^{-3} mm^2/s for WNT medulloblastomas ($P = .02$ and .13). The median ratio of ADC values in the EST or the WT to normal cerebellar tissue was highest for group 3/group 4 and lowest for WNT medulloblastomas ($P = .03$ and .09), with similar results in pairwise comparisons of the corresponding thalamic ADC values ($P = .02$ and .06).

CONCLUSION: ADC analysis of a tumor's contrast-enhancing solid portion may aid preoperative molecular classification/prediction of pediatric medulloblastomas and may facilitate optimal surgical treatment planning, reducing surgery-induced morbidity.

Keywords: Apparent diffusion coefficient, diffusion-weighted imaging, medulloblastoma, molecular groups, posterior fossa tumors.

Acceptance: Received September 24, 2019, and in revised form February 13, 2020. Accepted for publication March 5, 2020.

Correspondence: Address correspondence to Zoltan Patay, Department of Diagnostic Imaging, MS 220, Room I3119, St. Jude Children's Research Hospital, 262 Danny Thomas Place, Memphis, TN 38105. E-mail: zoltan.patay@stjude.org.

Acknowledgements and Disclosure:This paper would not have been possible without the support and expertise of our friend and colleague Dr. Andrea Poretti whose untimely death will always be incomprehensible to us. Dr. Poretti will be remembered for his passion to help children with neurological diseases, discover new diseases, and his exceptional dedication to teaching and mentoring young investigators. He would have been one of the significant contributing authors of this manuscript. The authors gratefully acknowledge the scientific editorial support provided by Cherise Guess, PhD.

K. A. Carson's work on the project was funded by the Johns Hopkins Institute for Clinical and Translational Research, under grant number UL1 TR001079 from the National Center for Advancing Translational Sciences, a component of the National Institutes of Health (NIH) and the NIH Roadmap for Medical Research.

The other authors declare no conflicts of interest to disclose relevant to the subject matter of this paper.

J Neuroimaging 2020;00:1-9.
DOI: 10.1111/jon.12704

Introduction

Medulloblastoma is a malignant brain tumor; this aggressive, invasive embryonal neoplasm accounts for 40% of childhood tumors in the posterior fossa.[1] In the United States, the overall incidence of medulloblastoma is around 1.5 per million people for the past 40 years. Although outcomes in children with medulloblastoma have improved significantly in the last decades, this group of pediatric brain tumors remains a substantial cause of severe morbidity and mortality in young children.[2]

Until recently, medulloblastomas were classified based primarily on histopathology, which included subtypes such as classic medulloblastoma, desmoplastic/nodular medulloblastoma, medulloblastoma with extensive nodularity, and large cell/anaplastic medulloblastoma.[2,3] The 2016 WHO classification of medulloblastoma accounts for demographic, clinical, transcriptional, and genetic differences of medulloblastomas, dividing them into four distinct groups: WNT activated (WNT), Sonic hedgehog activated (SHH), group 3, and group 4. The differentiation between medulloblastoma groups has been increasingly used for risk-stratified management decisions to improve outcomes and reduce therapy-related morbidities.[4-7]

With the advent of robust immunohistochemistry methods, molecular group information is increasingly available after surgery for medulloblastoma and is recognized as the new standard for risk stratification in all clinical settings.[4,9] A similar, broadly useable, robust, and reproducible approach to presurgical molecular classification, however, may be valuable at the time of the initial diagnostic imaging workup and operative planning. Because magnetic resonance imaging (MRI) of the brain is universally performed as the initial diagnostic imaging

evaluation of patients with brain tumors, including medulloblastomas, MRI-based, preferably quantitative biomarkers would be of benefit.

Conventional MRI may provide some clues for molecular grouping using features such as location and contrast enhancement after intravenous gadolinium-based contrast injection.[8,10,11] However, diffusion-weighted imaging (DWI) has been shown to allow differentiation among medulloblastoma and other common nonembryonal tumors (ependymoma and juvenile pilocytic astrocytoma) in the posterior fossa on the basis of differences in apparent diffusion coefficient (ADC) values. Correlations between ADC values and histopathological phenotypes are also suggested: for example, higher mean ADC values were found to be more characteristic of large-cell/anaplastic medulloblastoma than of classic medulloblastoma.[10]

Capitalizing on a relatively large patient cohort with available molecular data, in this study, we report ADC values acquired by using two region-of-interest (ROI)-based approaches in pediatric medulloblastomas, the results of statistical analysis to test for possible correlation between those values, and available immunohistochemistry-based molecular grouping data.

Methods

Retrospective review of the patients' medical files was conducted after approval and waiver-of-consent obtained from the institutional research boards of all participating institutions.

Subjects

The inclusion criteria for this study were as follows: (1) diagnosis of medulloblastoma under 18 years of age; (2) availability of molecular group assignment; and (3) availability of ADC map images of the tumor. Eligible patients were identified through an electronic search of the pediatric neuroradiology databases of the participating tertiary children's hospitals for the time period of January 2008 to February 2016.

MRI Data Acquisition

All MRI studies were performed on 1.5-T scanners (Siemens Avanto, Erlangen, Germany) by using standard departmental pediatric tumor protocol including isotropic gradient-echo T1-weighted images; axial T2-weighted and T2-FLAIR images; and axial, coronal, and sagittal T1-weighted images after intravenous injection of gadolinium-based contrast agent. DWI sequences were acquired by using a diffusion-weighted single-shot echo-planar sequence with diffusion gradients along the *X*-, *Y*-, and *Z*-axes and effective *b*-values of 0 and 1,000 s/mm^2, but some sequence parameters were slightly different at the three participating institutions. At institution 1 and 2, scan parameters were as follows: TR, 8,000 ms; TE, 91 ms; matrix 192 × 92; field of view, 240 mm × 240 mm; and slice thickness, 3 mm. At institution 3, scan parameters were as follows: TR, 10,000 ms; TE, 100 ms; matrix, 128 × 100; field of view, 230 × 100 mm; and slice thickness, 3 mm. ADC maps were automatically calculated by the vendor-specific in-line software on the MRI scanners. DWI was always performed before intravenous contrast injection.

Image Analysis

Image analysis was performed on the picture-archiving and communication system workstation in each institution. We used methods similar to Poretti et al's to measure ADC values[12] (Figs 1 and 2). The person placing the ROI for all studies was blinded to the conventional histopathology and molecular data. First, the enhancing, solid portion of the tumor (EST) was identified on contrast-enhanced axial T1-weighted images and correlated with the matching ADC maps. ROIs of 40-100 mm^2 were placed in the area corresponding to the EST on the ADC maps, as previously described.[12] Subsequently, the whole tumor (WT) was identified on axial T2-weighted and T2-weighted fluid-attenuated inversion recovery images and matching ADC maps. ROIs were placed to cover the WT, including enhancing and nonenhancing solid, as well as cystic lesion components. Peritumoral edema was excluded. For both measurements, three different ROIs were placed in the tumors on three representative contiguous MRI slices. The median (or "absolute") ADC value was calculated for each tumor. One ROI of approximately 115-125 mm^2 was placed within the normal-appearing cerebellar tissue (including both gray and white matter) to obtain a control cerebellar ADC value (Fig 3), and two ROIs of approximately 50-60 mm^2 were placed in both thalami (easily and readily identifiable structure on ADC map images and usually considered to be resistant to possible changes related to hydrocephalus). The average thalamic ADC values were calculated to obtain a second control ADC value. Finally, the ratios between the ADC values of the tumors (EST and WT separately) and the cerebellar and thalamic control ADC values were calculated.

We also calculated means and standard deviations for each of the "reference" measures (cerebellum, L thalamus, R thalamus, and thalamus average) to compute percent coefficients of variation (defined as the SD/mean).

Molecular Group Information

Molecular group data were acquired from the electronic medical records at the participating institutions. Medulloblastomas were categorized as WNT, SHH, or non-WNT/non-SHH (ie, group 3 and 4 combined). Molecular group was determined by immunohistochemistry.[9]

Statistical Analysis

Nonparametric methods were used to summarize and compare the data across molecular or histopathologic groups because most measures were not normally distributed. Demographic and clinical characteristics were summarized with counts and percentages or medians and interquartile ranges (IQRs). Fisher's exact tests were used to compare categorical data across the three molecular groups. Three group comparisons for continuous measures were made using the Kruskal-Wallis test. For the significant three-group comparisons, pairwise comparisons were conducted using the Wilcoxon rank sum test to identify which groups differed. We performed analyses using SAS version 9.3 and 9.4 (SAS Institute, Inc. Cary, NC, USA). All tests were two-sided, and significance was set at $P < .05$. No adjustment was made for multiple comparisons.

Results

The inclusion criteria were fulfilled for 93 children (65 males). The median age at presurgical MRI was 7 years (IQR, 4-10 years). Demographic and clinical features are presented

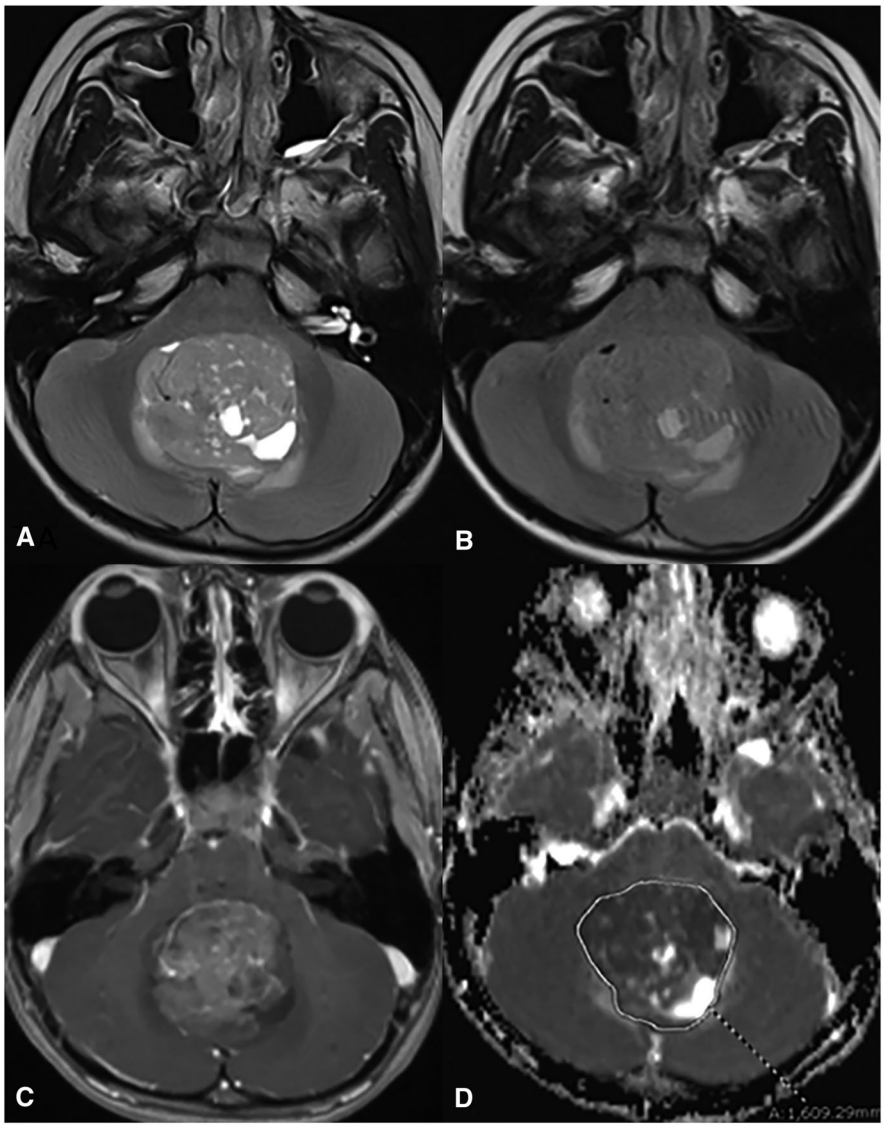

Fig 1. Sample region of interest (ROI) placement in the Whole Tumor. Axial T2-weighted (A) and fluid-attenuated inversion recovery (B) images show a large, midline, intraventricular solid mass with heterogeneous signal. Axial contrast-enhanced T1-weighted image at the same level as (A) and (B) demonstrates heterogeneous enhancement (C). ROI is drawn outlining the entire tumor on the apparent diffusion coefficient map (D).

in Table 1. Fifty-seven children (61%) had group 3/group 4 (Fig 4), 27 (29%) had SHH (Fig 5), and 9 (10%) had WNT medulloblastomas (Fig 6).

Median (IQR) absolute ADC values and ratios by molecular groups are presented in Table 2. The median (IQR) absolute ADC values in EST and WT were .719 (.632-.818) $\times 10^{-3}$ and .864 (.788-1.068) $\times 10^{-3}$ mm^2/s for group 3/group 4, .660 (.574-.797) $\times 10^{-3}$ and .965 (.735-1.130) $\times 10^{-3}$ mm^2/s for SHH, and .594 (.573-.675) $\times 10^{-3}$ and .728 (.617-.841) $\times 10^{-3}$ mm^2/s for WNT medulloblastomas ($P = .02$ and .13) (Fig 7).

The median (IQR) ratio of ADC values in EST and in WT to that in normal cerebellar tissue was 1.017 (.874-1.104) and 1.258 (1.090-1.411) for group 3/group 4, .895 (.826-1.024) and 1.291 (1.038-1.625) for SHH, and .888 (.815-.928) and 1.029 (.902-1.184) for WNT medulloblastomas ($P = .03$ and .09) (Fig 8).

The median (IQR) ratio of ADC values in EST and in WT to that in normal thalamic tissue was .922 (.800-1.066) and 1.126 (.991-1.342) for group 3/group 4, .791 (.744-.933) and 1.155 (.979-1.381) for SHH, and .754 (.661-.839) and .936 (.808-1.015) for WNT medulloblastomas ($P = .02$ and .06) (Fig 9).

The median (IQR) absolute ADC values and ratios by conventional histopathology categories are presented in Table 3. We found none of the absolute ADC measures and ratios in EST or WT to be different across histopathology groups.

Percent coefficients of variation for the reference measurements in the cerebellum and thalami were consistently around 14%, which is usually considered "good precision."

Pairwise Comparisons

The absolute ADC values in the EST were highest in group 3/group 4 and significantly differed from those of WNT (.7268 vs. .5824; $P = .01$), which had the lowest ADC values. The ratio of ADC values in EST to those in normal cerebellum was highest in Group 3/Group 4 (1.0293), which differed from both SHH (.9558; $P = .049$) and WNT (.8837; $P = .03$). Similarly,

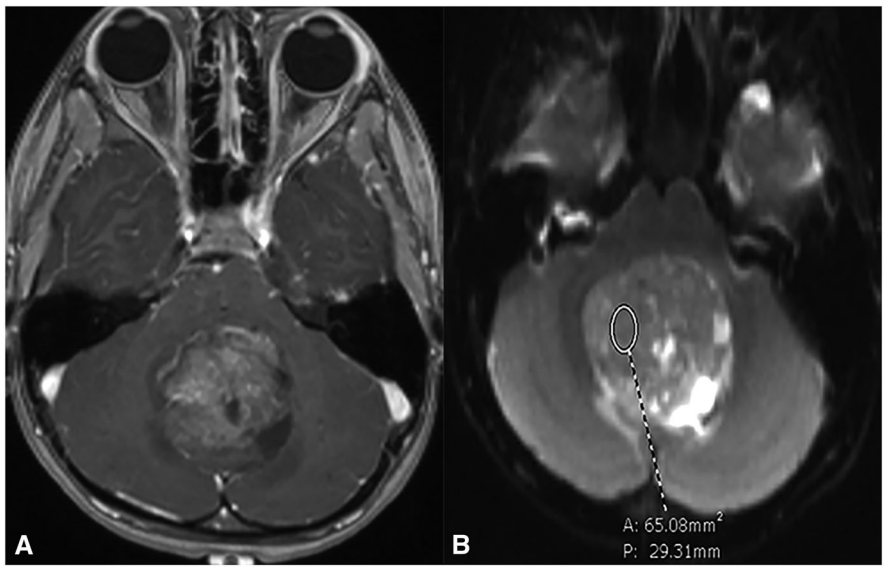

Fig 2. Sample region of interest (ROI) placement in the enhancing solid tumor. Axial contrast-enhanced T1-weighted image demonstrates heterogeneous enhancement (A). ROI is drawn on enhancing solid tumor on the apparent diffusion coefficient map (B).

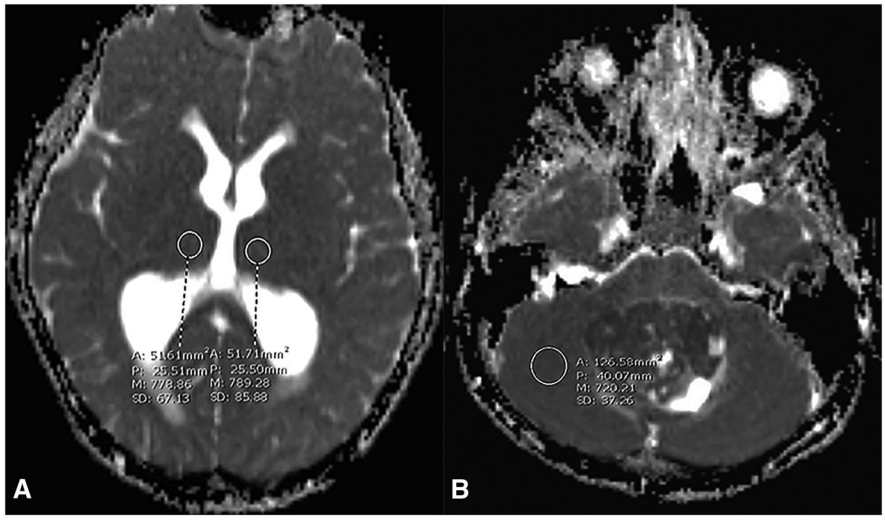

Fig 3. Sample region of interest (ROI) placement for control values in thalami and cerebellum. ROI placed on both thalami on the apparent diffusion coefficient (ADC) map (A). ROI placed in the normal cerebellar tissue on the ADC map (B).

Table 1. Demographic and Clinical Characteristics of Medulloblastoma Patients

	Molecular Group			
Characteristic	**SHH (*N* = 27)**	**WNT (*N* = 9)**	**Group 3/4 (*N* = 55)**	***P*-value[a]**
Age in years, median (interquartile range)	3 (2-10)	10 (9-11)	7 (5-10)	.003
Sex				.79
Male	18 (67%)	6 (67%)	41 (72%)	
Female	9 (33%)	3 (33%)	16 (28%)	
Site				.96
Emory University	4 (15%)	1 (11%)	8 (14%)	
Johns Hopkins Hospital	1 (4%)	0 (0%)	1 (2%)	
St Jude Children's Research Hospital	22 (81%)	8 (89%)	48 (84%)	
Pathology group				<.001
Anaplastic	1 (4%)	0 (0%)	13 (23%)	
Classic	4 (15%)	9 (100%)	44 (77%)	
Desmoplastic	22 (81%)	0 (0%)	0 (0%)	

N = number of subjects.
[a]All P values determined via Fisher's exact test, except age, which was via Kruskal-Wallis test.

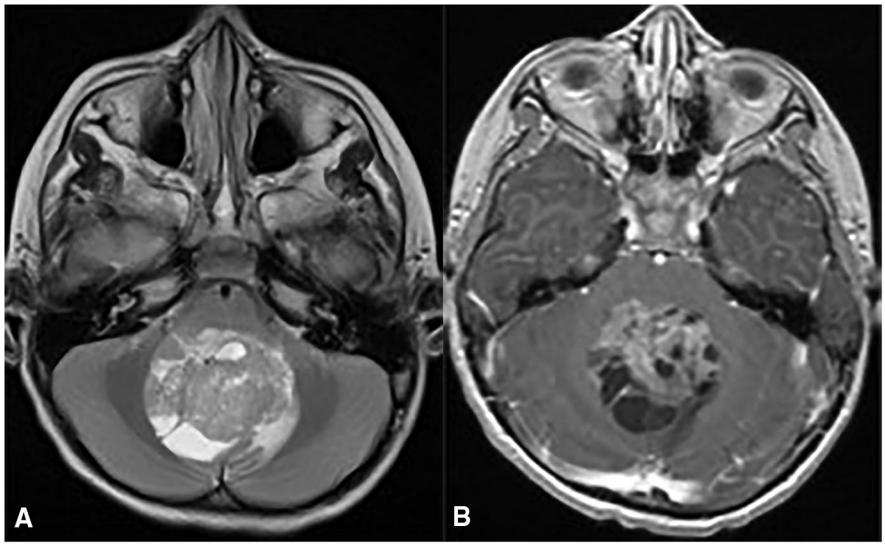

Fig 4. SHH tumor. T2-weighted axial MRI showing a heterogeneous T2-hyperintense mass lesion in the midline with intrinsic and peripheral cystic areas (A). Axial contrast-enhanced T1-weighted MRI at the same level reveals heterogeneous enhancement (B).

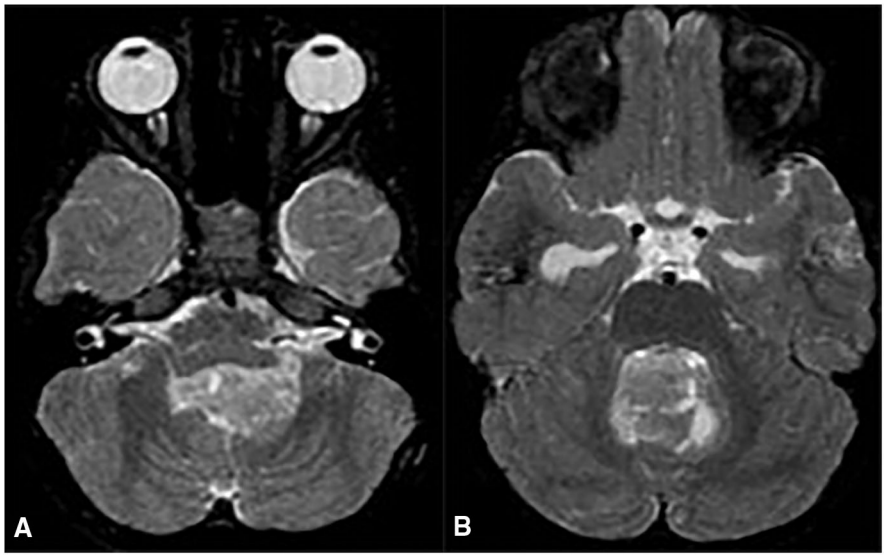

Fig 5. WNT tumor. T2-weighted axial MR images show a heterogeneous hyperintense mass in the fourth ventricle extending into the left foramen of Luschka.

the ratio of ADC values in EST to those in normal thalamus was highest in Group 3/Group 4 (.9304), significantly differing from the ratios in both SHH (.8519; $P = .046$) and WNT (.7584; $P = .01$).

Discussion

Medulloblastomas have four distinct molecular groups based on gene expression or DNA methylation profiling (WNT, SHH, group 3, and group 4). Compared to conventional tumor histology (ie, classic and variants, such as desmoplastic, large cell/anaplastic, and extensive nodularity), these groups are better correlated with clinical features, imaging characteristics, and outcomes.[4,5,13] For example, group 3/4 tumors always develop in the fourth ventricle, whereas WNT tumors predominantly occur within the foramen of Luschka or cerebrospinal fluid-filled spaces adjacent to that (fourth ventricle, cisterna magna, and cerebellopontine angle cistern). SHH medulloblastomas are characteristically hemispheric and, more rarely, may be in the midline, including the fourth ventricle.[6,11] Location is a useful imaging feature but, unfortunately, there is a spatial overlap of all four molecular groups in the fourth ventricle, which is the most common, "classic" location of medulloblastomas in about 75% of patients.[4,14]

Molecular grouping data are the core of all current risk-stratification schemes, although typically used with other factors (metastatic status, TP53 mutation, MYC amplification, chromosome 13 loss, etc) to maximize survival and minimize treatment-related side effects.[15,16] Because MRI, including advanced MRI sequences such as DWI with calculation of ADC maps, is systematically used in most pediatric healthcare facilities, objective, noninvasive quantitative evaluation of posterior fossa tumors, suspected to correspond to medulloblastoma, is already achievable before

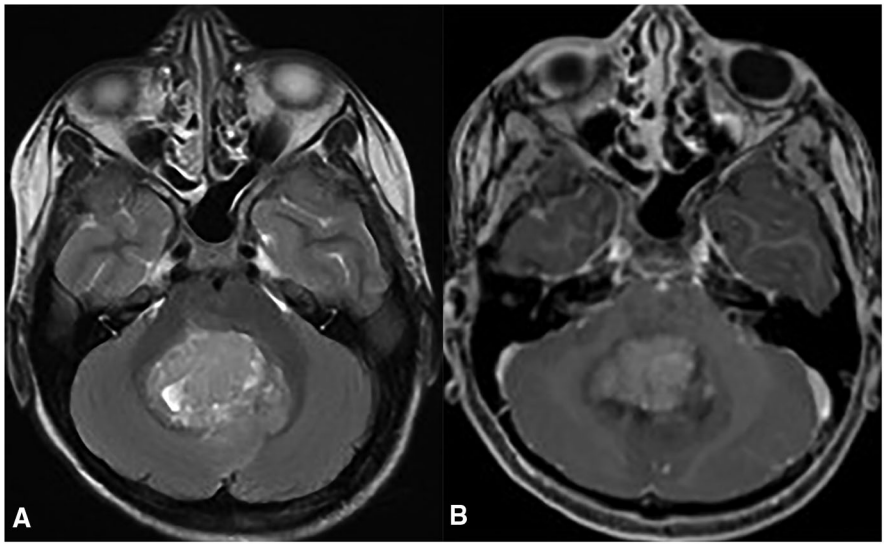

Fig 6. Non-SHH/non-WNT tumor. T2-weighted axial MR image showing mixed intense signal in midline, intraventricular tumor in the posterior fossa (A). Axial contrast-enhanced T1-weighted MR image at the same level reveals moderate enhancement (B).

Table 2. Median Medulloblastoma Apparent Diffusion Coefficient (ADC) Measurements and Ratios

	Molecular Group			
Measure	SHH ($N = 27$)	WNT ($N = 9$)	Group 3/4 ($N = 55$)	*P*-value[a]
Absolute ADC in enhancing solid tumor, $\times 10^{-3}$ mm^2/s	.660 (.574-.797)	.594 (.573-.675)	.719 (.632-.818)	.02[b]
Absolute ADC in whole tumor, $\times 10^{-3}$ mm^2/s	.965 (.735-1.130)	.728 (.617-.841)	.864 (.788-1.068)	.13
Cerebellar ratio in enhancing solid tumor	.895 (.826-1.024)	.888 (.815-.928)	1.017 (.874-1.104)	.03[c]
Cerebellar ratio in whole tumor	1.291 (1.038-1.625)	1.029 (.902-1.184)	1.258 (1.090-1.411)	.09
Thalamic ratio in enhancing solid tumor	.791 (.744-.933)	.754 (.661-.839)	.922 (.800-1.066)	.02[d]
Thalamic ratio in whole tumor	1.155 (.979-1.381)	.936 (.808-1.015)	1.126 (.991-1.342)	.06

N = number of subjects.
[a] *P*-value is from the Kruskal-Wallis test comparing all three groups.
[b] On pairwise comparison, Group 3/4 differed from WNT ($P = .01$).
[c] On pairwise comparison, Group 3/4 differed from both SHH ($P = .049$) and WNT ($P = .03$).
[d] On pairwise comparison, Group 3/4 differed from both SHH ($P = .046$) and WNT ($P = .01$).

surgery with a high level of confidence.[17] This approach may allow preliminary prognostication and enhanced surgical planning.

In this retrospective research, our aim was to assess the value of ADC sampling across the molecular groups to find a simple, reproducible, quantifiable, and user-independent tool for MRI-based prediction of molecular medulloblastoma groups. We used both absolute ADC values and ratios, which are easier to measure/calculate in daily clinical work and are likely to correct for variability in patient age (hence brain maturation), as well as scanner and imaging acquisition variability; the latter are unavoidable in collaborative multicenter retrospective studies, like ours. ADC ratios have also been used in multicentric studies to compare data among different institutions.[18]

In several previous studies, including one conducted by Poretti et al,[10] the ADC values were significantly higher in low-grade than in high-grade tumors, reflecting the different intratumoral cellular densities according to tumor grade. In a study by Gauvain et al,[19] ADC ratio (tumor vs. normal-appearing cerebellar tissue) and histologic classification correlated well in five pediatric posterior fossa tumors. A similar approach was used in our study.

In biological specimens, ADC values are determined by the proportions of intracellular and extracellular water compartments. High cellularity and high nuclear-to-cytoplasmic ratio are associated with low ADC values. A more facilitated water motion in the interstitial space may contribute to higher ADC values.[19] Consequently, in classic medulloblastomas where cells are very small and firmly packed with scant cytoplasm, reduced water motion or greater water restriction presents with relatively low ADC values. In anaplastic or large-cell medulloblastoma, the tumor cells are larger and less tightly packed, resulting in higher ADC values.[10,20,21]

In studies conducted by Northcott et al[4] and Kool et al,[22] all (9/9) WNT tumors were described as classic medulloblastomas, and most (22/27) SHH tumors were desmoplastic. In the study conducted by Ellison et al,[9] most (44/58) group 3/4 medulloblastomas were classic, and the rest (11/58) were anaplastic/large-cell variant.

In our study, Group 3/4 tumors showed the highest median ADC values in the EST, the highest ratio of EST ADC values to normal cerebellum ADC values, and the highest ratio of EST ADC values to normal thalamus ADC values, which may be explained by the fact that they have the highest percentage of

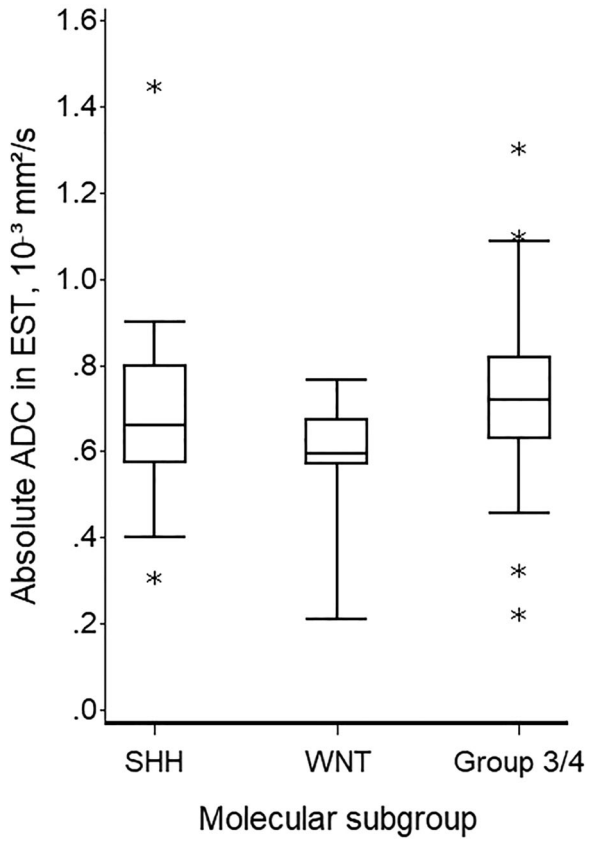

Fig 7. Scatter diagram of absolute apparent diffusion coefficient (ADC) values in enhancing solid part of the tumor (EST) for all molecular groups.

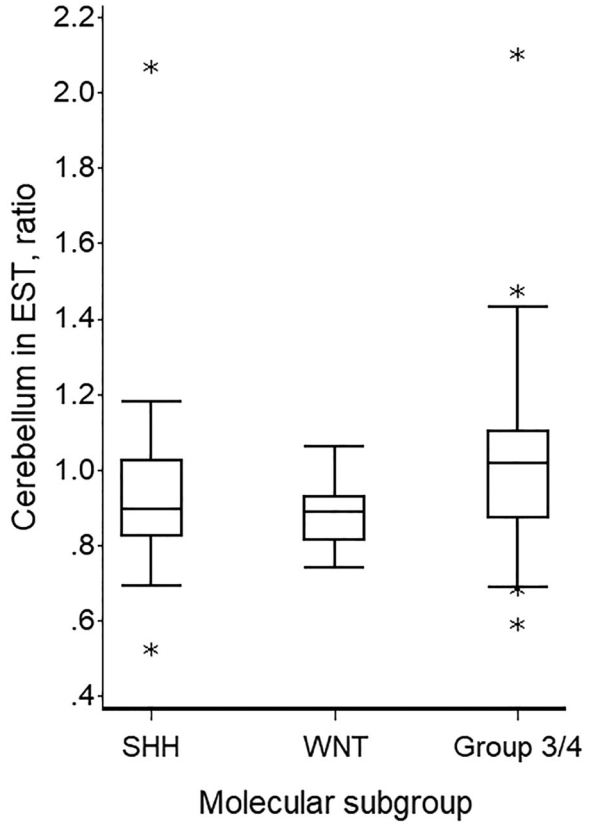

Fig 8. Scatter diagram of ADC ratios of enhancing, solid part of the tumor (EST) to normal cerebellar tissue for all molecular groups.

the anaplastic variant among the tumors in the study group. In contrast, the WNT tumors consisted entirely of the classic medulloblastoma variant and had the lowest median ADC values in the EST and the lowest ratios of EST ADC values to ADC values in normal cerebellum or normal thalamus, which can be explained by the high nucleus to cytoplasm ratio and densely packed small cells in this group.[21,22,23] SHH tumors had intermediate values across all three comparisons, which could be due to the heterogeneous histopathological presentation with all three histopathological variants represented in these tumors in our study population. The ADC values being somewhat closer to the WNT tumors could be because, in most of the desmoplastic medulloblastomas (maximum presentation in our study group of SHH tumors; 22/27), the extracellular water motion is likely restricted by dense reticulin fibers, resulting in low ADC values.[10,24,25]

The absolute ADC values for the WT and ADC ratios (WT/normal cerebellum and WT/normal thalamus) did not show statistically significant correlation, which could be due to often prominent intratumoral heterogeneities in these tumors, such as hemorrhage, edema, necrosis, and cysts.[10,12]

We acknowledge limitations to our study. The total number of patients may be relatively high but is not uniformly distributed for every histological subtype and included pediatric patients only. Although areas of cysts, gross necrosis, and hemorrhage were excluded as much as possible while measuring the ADC values of the EST, microscopic necrosis and intratumoral variation in cell size certainly contribute to

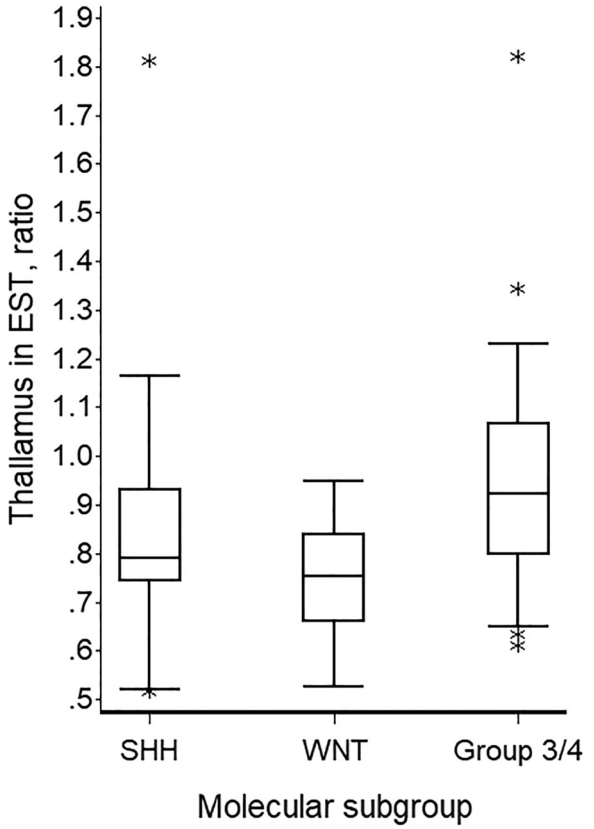

Fig 9. Scatter diagram of ADC ratios of enhancing solid part of the tumor (EST) to normal thalamus for all molecular groups.

Table 3. Median (Interquartile Range) Medulloblastoma ADC Measurements and Ratios by Histopathology Subgroup

Measure	Histopathology subgroups			
	Anaplastic ($N = 14$)	Classic ($N = 57$)	Desmoplastic ($N = 22$)	P-value[a]
Absolute ADC in Enhancing solid tumor (EST), $\times 10^{-3}$ mm^2/s	0.712 (0.632-0.807)	0.700 (0.594-0.781)	0.660 (0.578-0.797)	0.60
Absolute ADC in Whole Tumor (WT), $\times 10^{-3}$ mm^2/s	0.965 (0.884-1.068)	0.846 (0.748-1.080)	0.927 (0.729-1.080)	0.20
Cerebellar ratio in Enhancing solid tumor (EST)	1.045 (0.842-1.143)	0.965 (0.860-1.067)	0.911 (0.860-1.011)	0.40
Cerebellar ratio in Whole Tumor (WT)	1.346 (1.253-1.515)	1.215 (1.040-1.411)	1.252 (1.038-1.443)	0.13
Thalamic ratio in Enhancing solid tumor (EST)	0.916 (0.820-1.066)	0.907 (0.751-0.989)	0.806 (0.758-0.933)	0.47
Thalamic ratio in Whole Tumor (WT)	1.211 (1.119-1.415)	1.040 (0.950-1.342)	1.150 (0.933-1.343)	0.13

[a] P-value is from the Kruskal-Wallis test comparing all 3 groups.

variations in cell density that would be expected to affect diffusion measurements. Moreover, our study was focused on only one imaging parameter for tumor differentiation. We did that because we wanted to use a robust, simple, widely available tool for tumor analysis. However, multiparametric analysis including data from magnetic resonance spectroscopy, perfusion-weighted imaging, diffusion-tensor imaging, and ADC histogram profiling may further increase the power of predicting molecular tumor group with greater accuracy.[26]

Because there is a considerable overlap in the distribution of ADC values/ratios between medulloblastoma groups, our method alone may not allow accurate group determination in each individual case. Furthermore, the immunohistochemical method used for group assessment in our cohort did not allow differentiation between group 3 and group 4 tumors. However, the use of DWI-based ADC analysis of tumors in conjunction with other robust and well-established group features (location and enhancement in particular) may permit a fairly confident group prediction at the initial diagnostic imaging evaluation of children with suspected medulloblastoma, which may be particularly useful in tumors located within the fourth ventricle where all four molecular medulloblastoma groups may be encountered. Preliminary molecular information may be a useful adjunct to discussions about prognosis with patients and families at the initial diagnosis, but it may have some implications for surgical planning, too. The current standard of surgical care for medulloblastoma is maximal safe tumor resection. Historically, residual tumor (>1.5 cm^2) has been associated with worse prognosis compared to that of patients undergoing gross total tumor resection (GTR).[26,27,28] This conclusion, however, has been challenged recently, and an increasing number of investigators believe that sub- or near-total tumor resection is acceptable in specific settings.[29] Although GTR has a statistically significant positive effect on overall survival in SHH medulloblastoma diagnosed in childhood, a similar correlation has not been found in group 3 and group 4 medulloblastomas.

In view of the fairly frequent (11-29%) development of postoperative cerebellar mutism syndrome in midline intraventricular medulloblastoma patients, preoperative determination of molecular groups may have implications on surgical strategies.[30]

Cerebellar mutism syndrome develops after bilateral surgical damage to the proximal efferent cerebellar pathways (dentate nuclei and superior cerebellar peduncles); therefore, sparing at least one of the two efferent cerebellar pathways even at the cost of leaving a small amount of residual tumor may be a consideration in putative group 3 and group 4 tumors. WNT tumors have invariably favorable prognosis, so sparing at least one of the efferent cerebellar pathways may not decrease survival in these patients either. Conversely, because failure in the form of local recurrence is most common in SHH medulloblastoma, gross-total tumor resection would confer survival benefit to group 2 medulloblastoma patients.

In summary, our study shows that assessing ADC values in solid enhancing, nonnecrotic, nonedematous tumor regions might allow differentiation of group 3/4 tumors from WNT and SHH groups, which may facilitate optimal treatment planning and reduce surgery-induced morbidity. These data should be used with other robust MRI features, such as enhancement and location. The combined use of these parameters and the metastatic status of the disease, if validated in larger series, may allow the development of an MRI-based prognostication and risk-prediction algorithm to be used preoperatively.

References

1. Partap S, Curran EK, Propp JM, et al. Medulloblastoma incidence has not changed over time: a CBTRUS study. J Pediatr Hematol Oncol 2009;31:970-1.
2. McManamy CS, Lamont JM, Taylor Roger E. Morphophenotypic variation predicts clinical behavior in childhood non-desmoplastic medulloblastomas. J Neuropathol Exp Neurol 2003;62:627-32.
3. Pomeroy SL, Tamayo P, Gaasenbeek M, et al. Prediction of central nervous system embryonal tumour outcome based on gene expression. Nature 2002;415:436-42.
4. Northcott PA, Korshunov A, Witt H, et al. Medulloblastoma comprises four distinct molecular variants. J Clin Oncol 2011;29: 1408-14.
5. Miranda Kuzan-Fischer C, Juraschka K, Taylor MD. Medulloblastoma in the molecular era. J Korean Neurosurg Soc 2018;61:292-301.
6. Taylor MD, Northcott PA, Korshunov A, et al. Molecular subgroups of medulloblastoma: the current consensus. Acta Neuropathol 2012;123:465-72.
7. Perreault S, Ramaswamy V, Achrol AS, Chao K, et al. MRI surrogates for molecular subgroups of medulloblastoma. AJNR Am J Neuroradiol 2014;35:1263-9.
8. Cavalli FMG, Remke M, Rampasek L, et al. Intertumoral heterogeneity within medulloblastoma subgroups. Cancer Cell 2017;31:737-54.e6.
9. Ellison DW, Dalton J, Kocak M, et al. Medulloblastoma: clinicopathological correlates of SHH, WNT, and non-SHH/WNT molecular subgroups. Acta Neuropathol 2011;121:381-96.
10. Poretti A, Meoded A, Thierry A G. Neuroimaging of pediatric posterior fossa tumors including review of the literature. J Magn Reson Imaging 2012;35:32-47.
11. Patay Z, DeSain LA, Hwang SN, et al. MR imaging characteristics of wingless-type–subgroup pediatric medulloblastoma. AJNR Am J Neuroradiol 2015;36:2386-93.

12. Poretti A, Meoded A, Cohen KJ, et al. Apparent diffusion coefficient of pediatric cerebellar tumors: a biomarker of tumor grade? Pediatr Blood Cancer 2013;60:2036-41.
13. Cho Y-J, Tsherniak A, Tamayo P, et al. Integrative genomic analysis of medulloblastoma identifies a molecular subgroup that drives poor clinical outcome. J Clin Oncol 2011;29:1424-30.
14. Ellison DW, Onilude OE, Lindsey JC, et al. β-Catenin status predicts a favorable outcome in childhood medulloblastoma: the United Kingdom Children's Cancer Study Group Brain Tumour Committee. J Clin Oncol 2005;23:7951-7.
15. Fattet S, Haberler C, Legoix P, et al. Beta-catenin status in paediatric medulloblastomas: correlation of immunohistochemical expression with mutational status, genetic profiles, and clinical characteristics. J Pathol 2009;218:86-94.
16. Gajjar A, Chintagumpala M, Ashley D, et al. Risk-adapted craniospinal radiotherapy followed by high-dose chemotherapy and stem-cell rescue in children with newly diagnosed medulloblastoma (St Jude Medulloblastoma-96): long-term results from a prospective, multicentre trial. Lancet Oncol 2006;7:813-20.
17. Robinson GW. Impact of tumor location on medulloblastoma subtyping and treatment. Pediatr Blood Cancer 2013;60:1393-4.
18. Huisman TA. Diffusion-weighted imaging: basic concepts and application in cerebral stroke and head trauma. Eur Radiol 2003;13:2283-97.
19. Gauvain KM, McKinstry RC, Mukherjee P, et al. Evaluating pediatric brain tumor cellularity with diffusion-tensor imaging. AJR Am J Roentgenol 2001;177:449-54.
20. Filippi CG, Lin DDM, Tsiouris Apostolos J. Diffusion-tensor MR imaging in children with developmental delay: preliminary findings. Radiology 2003;229:44-50.
21. Kono K, Inoue Y, Nakayama K, et al. The role of diffusion-weighted imaging in patients with brain tumors. AJNR Am J Neuroradiol 2001;22:1081-8.
22. Kool M, Koster J, Bunt J, et al. Integrated genomics identifies five medulloblastoma subtypes with distinct genetic profiles, pathway signatures and clinicopathological features. PLoS ONE 2008;3:e3088.
23. Bihan DL, Le Bihan D, Breton E, et al. MR imaging of intravoxel incoherent motions: application to diffusion and perfusion in neurologic disorders. Radiology 1986;161:401-7.
24. Liu H-Q, Yin X, Li Y, et al. MRI features in children with desmoplastic medulloblastoma. J Clin Neurosci 2012;19:281-5.
25. Pillai S, Singhal A, Byrne AT, et al. Diffusion-weighted imaging and pathological correlation in pediatric medulloblastomas - "they are not always restricted!". Childs Nerv Syst 2011;27:1407-11.
26. Schob S, Beeskow A, Dieckow J, et al. Diffusion profiling of tumor volumes using a histogram approach can predict proliferation and further microarchitectural features in medulloblastoma. Childs Nerv Syst 2018;34:1651-6.
27. Albright AL, Leland Albright A, Wisoff Jeffrey H. Effects of medulloblastoma resections on outcome in children: a report from the Children's Cancer Group. Neurosurgery 1996;38:265-71.
28. Zeltzer PM, Boyett JM, Finlay JL, et al. Metastasis stage, adjuvant treatment, and residual tumor are prognostic factors for medulloblastoma in children: conclusions from the Children's Cancer Group 921 Randomized Phase III Study. J Clin Oncol 1999;17:832-45.
29. Thompson EM, Hielscher T, Bouffet E, et al. Prognostic value of medulloblastoma extent of resection after accounting for molecular subgroup: a retrospective integrated clinical and molecular analysis. Lancet Oncol 2016;17:484-95.
30. Gudrunardottir T, Sehested A, Juhler M, et al. Cerebellar mutism: definitions, classification and grading of symptoms. Childs Nerv Syst 2011;27:1361-3.